ELSEVIER

Journal of Organometallic Chemistry 529 (1997) 143–149

Journal of Organometallic Chemistry

Phosphaalkene derivatives of furane and thiophene: synthesis, crystal structure, electrochemistry and EPR study of their radical anions

A. Jouaiti [a], A. Al Badri [a], M. Geoffroy [a,*], G. Bernardinelli [b]

[a] *Department of Physical Chemistry, University of Geneva, 30 quai E. Ansermet, 1211 Geneva, Switzerland*
[b] *Laboratory of Crystallography, University of Geneva, 24 quai E. Ansermet, 1211 Geneva, Switzerland*

Received 4 April 1996; revised 10 May 1996

Abstract

Two phosphaalkenes containing either a furane or a thiophene ring bound to the carbon atom of the –P=C< bond have been synthesized. The crystal structure of the furane derivative has been determined and the electrochemistry of both compounds has been investigated. THF solutions of these compounds react at 255 K with a potassium mirror to yield the corresponding radical anions which have been studied by EPR in both the liquid and solid states. The resulting hyperfine constants are compared with the values predicted by ab initio calculations on radical anions formed from model phosphaalkenes.

Keywords: Phosphaalkene; Electron spin resonance; Electrochemistry; Crystal structure; Radical anion

1. Introduction

Since the pioneering work on the stabilization of compounds containing a trivalent dicoordinated phosphorus atom [1,2], numerous studies [3–10] have been devoted to the properties of the –P=C< bond. For example, electrochemical investigations have shown that reduction of phosphaalkene moieties is strongly dependent upon the nature of the organic groups R bound to the phosphaalkenic carbon: this reduction is irreversible when R is an alkyl group [11] but is quasi-reversible when R is a phenyl group [12,13]. In this latter case, EPR spectra of the radical anion could be obtained, and it was shown that the unpaired electron was delocalized in a π^* orbital composed of a phosphorus 3p-orbital and carbon 2p-orbitals of both the phosphaalkene and the benzene groups. Owing to its orientation perpendicular to the C–P–C plane [13,14], the aromatic ring, Ar, bound to the phosphorus atom did not participate in this orbital. In the present work our purpose was to synthesize novel phosphaalkene molecules whose C–P=C carbon is bound to a heterocycle and to determine to what extent the heterocycle contributes to the SOMO of the corresponding radical anion. After synthesis of the compounds **1** and **2** and study of their electrochemical behavior, we have generated their radical anions, chemically, at 200 K and interpreted their EPR spectra obtained in both the liquid and solid states.

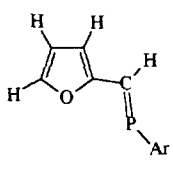

1

Ar: $C_6H_2{}^tBu_3$ - 2,4,6

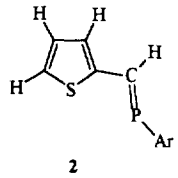

2

2. Experimental section

2.1. Compounds

All the syntheses were performed under an inert atmosphere, and all the solvents were distilled and degassed just before the experiment. $ArPH_2$ was synthesized according to a previously-reported procedure [15], 2-furaldehyde and 2-thiophene carboxaldehyde were purchased from Aldrich.

* Corresponding author.

PII S0022-328X(96)06526-6

The synthesis of the phosphaalkene moiety group was carried out following a method similar to that of Yoshifuji et al. [16]. 0.9 ml of a solution (1.6 M) of ^{n}BuLi in hexane was added to a solution of $ArPH_2$ (0.4 g) in THF. $^{t}BuMe_2SiCl$ (0.22 g) was added to the solution and an equivalent of ^{n}BuLi was added to the mixture. Then 0.2 ml of 2-furaldehyde was added to the solution, the mixture was stirred overnight and evaporated to dryness. The resulting phosphaalkene **1** was purified on a column using hexane as eluant. A similar method was used for the preparation of **2**, but in this case we used 2-thiophene carboxaldehyde as reagent.

Replacement of the phosphaalkenic proton of **1** by a deuterium (compound **D-1**) was performed by using the deuterated aldehyde $(C_4H_3O)C(D)O$ as reagent.

Analytical data. NMR spectra were recorded on a Bruker AC-200F (^{1}H, 200 MHz; ^{31}P, 81 MHz) spectrometer. External H_3PO_4 was used as reference. **1**: m.p. 138–140 °C; $^{31}P\{^1H\}$ NMR ($CDCl_3$) δ = 242.7 ppm; ^{1}H NMR ($CDCl_3$) 7.68 (d, 1H, H–C=P, J_{H-P} = 24.4 MHz); 6.22 (m, 1H, C_2–H), 6.41 (m, 1H, C_3–H), 7.43 (m, 1H, C_4–H); 7.427 and 7.434 (2H, Ar–H); 1.50 (s, 18H, Ar *ortho*-^{t}Bu), 1.25 (s, 9H, Ar *para*-^{t}Bu) ppm. **2**: m.p. 97–100 °C; $^{31}P\{^1H\}$ NMR ($CDCl_3$) δ = 246.4 ppm; ^{1}H NMR ($CDCl_3$) 8.1 (d, 1H, H–C=P, J_{H-P} = 25 Hz); 6.95 (m, 1H, C_2–H), 6.96 (m, 1H, C_3–H), 7.26 (m, 1H, C_4–H); 7.43 and 7.44 (2H, Ar–H); 1.50 (18H, Ar *ortho*-^{t}Bu); 1.25 (9H, Ar *para*-^{t}Bu).

2.2. Electrochemistry

Electrochemical measurements were carried out at room temperature (for **2**) and at 255 K (for **1**) using a BAS voltammograph (Model CV-50W). Cyclic voltammograms were obtained using a platinum electrode and an SCE reference with tetrabutylammonium hexafluorophosphate (10^{-1} M) as electrolyte and THF and DMF as solvents.

2.2.1. Crystal structure determination of D-1

$C_{23}H_{32}DOP$, M_r = 357.5; μ = 1.18 mm^{-1}, $F(000)$ = 776, d_x = 1.11 g cm^{-3}, monoclinic, $P2_1/n$, Z = 4, a = 9.563(1), b = 9.652(1), c = 23.113(2) Å, β = 90.385(4)°, V = 2133.3(4) Å^3 from 24 reflections (41° < 2θ < 66°), colorless prism 0.17 × 0.17 × 0.30 mm mounted on a quartz fiber. Cell dimensions and intensities were measured at 200 K on an Enraf–Nonius CAD4 diffractometer with graphite-monochromated Cu Kα radiation (λ = 1.5418 Å), ω–2θ scans, scan width 1.5° + 0.14 tg θ, scan speed 0.092° s^{-1}. Two reference reflections measured every 30 min showed a variation of less than 2.8$\sigma(I)$. 2524 measured reflections, 2457 unique reflections of which 2259 were observable ($F_o > 4\sigma(F_o)$); R_{int} for equivalent reflections 0.014. Data were corrected for Lorentz and polarization effects and for absorption [17] (A^* min., max. 1.213, 1.282). The structure was solved by direct methods using MULTAN 87 [18], all other calculations used the XTAL system [19] and ORTEP programs [20]. Full-matrix least-squares refinement based on F using a weighting of $1/\sigma^2(F_o)$ gave final values of R = 0.040, wR = 0.033 for 326 variables and 2259 contributing reflections. All coordinates of hydrogen atoms were observed and refined with U_{iso} fixed at 0.05 Å^2. The deuterium atom was refined with hydrogen atomic scattering factors. The final difference electron density map showed a maximum of +0.32 and a minimum of −0.30 e Å^{-3}.

2.3. Electron paramagnetic resonance

EPR spectra were recorded on a Bruker 200D spectrometer (X-band, 100 kHz field modulation) equipped with a variable temperature attachment.

All the liquid phase spectra were analyzed by comparing the experimental spectra with those obtained by simulation. The frozen solution spectra were simulated using a program which calculates the position of the resonance lines with second order perturbation and sums the resulting spectra obtained for 120 000 random orientations. The EPR samples were prepared by reacting, under high vacuum, a carefully degassed solution of phosphaalkene in THF on a freshly prepared mirror of potassium. This reaction was carried out at low temperature, and the tube was transferred, without warming, to the Dewar of the resonance cavity of the spectrometer.

2.4. Ab initio calculations

The quantum mechanic calculations were performed on a Silicon Graphics computer (IRIS 4D) with the Gaussian 92 [21] or Gaussian 94 [22] package. All calculations were carried out using the 6 − 31 + G basis set together with the ROHF method. The $\langle S^2 \rangle$ values

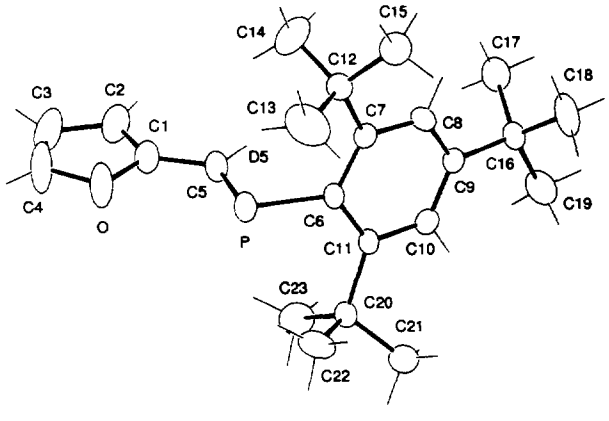

Fig. 1. Perspective view of the crystal structure of **D-1** with atomic numbering. Ellipsoids are represented with 50% probability.

Table 1
Atomic coordinates and equivalent isotropic displacement parameters ($Å^2$) with e.s.d.s in parentheses for compound **D-1**

Atom	x	y	z	U_{eq}
P	0.18185(7)	0.28144(7)	0.42708(3)	0.0339(2)
O	0.1304(2)	0.0772(2)	0.52514(8)	0.0560(8)
C(1)	0.2678(3)	0.1050(3)	0.5148(1)	0.035(1)
C(2)	0.3477(3)	0.0284(3)	0.5509(1)	0.043(1)
C(3)	0.2563(4)	−0.0506(3)	0.5852(1)	0.057(1)
C(4)	0.1296(4)	−0.0194(4)	0.5688(1)	0.067(1)
C(5)	0.2994(3)	0.2023(3)	0.4696(1)	0.0316(9)
C(6)	0.3036(2)	0.3826(2)	0.38155(9)	0.0238(8)
C(7)	0.3712(2)	0.3178(2)	0.33387(9)	0.0239(8)
C(8)	0.4943(2)	0.3779(3)	0.3141(1)	0.0276(9)
C(9)	0.5497(2)	0.5003(2)	0.33610(9)	0.0244(8)
C(10)	0.4680(2)	0.5704(3)	0.3760(1)	0.0274(9)
C(11)	0.3445(2)	0.5172(2)	0.39882(9)	0.0221(8)
C(12)	0.3171(2)	0.1871(2)	0.3018(1)	0.0300(9)
C(13)	0.1565(4)	0.1864(4)	0.2980(2)	0.070(2)
C(14)	0.3703(4)	0.0554(3)	0.3299(1)	0.062(1)
C(15)	0.3649(3)	0.1867(3)	0.2389(1)	0.044(1)
C(16)	0.6925(2)	0.5521(2)	0.3155(1)	0.0295(9)
C(17)	0.8043(3)	0.4453(3)	0.3321(1)	0.042(1)
C(18)	0.6925(3)	0.5679(4)	0.2499(1)	0.049(1)
C(19)	0.7338(3)	0.6892(3)	0.3435(2)	0.059(1)
C(20)	0.2600(2)	0.6095(2)	0.44103(9)	0.0275(9)
C(21)	0.2940(3)	0.7629(3)	0.4318(1)	0.045(1)
C(22)	0.1015(3)	0.5986(3)	0.4298(1)	0.052(1)
C(23)	0.2930(4)	0.5744(3)	0.5040(1)	0.056(1)

U_{eq} is the average of eigenvalues of U.

found for $1'^{\cdot-}$ and $2'^{\cdot-}$ with the UHF method were greater than 0.75.

3. Results

3.1. Crystal structure

The crystal structure of **D-1** was determined in order to know if the main characteristics of the phosphaalkene were perturbed by the presence of the heteroatom in the vicinity of the phosphorus atom. An ORTEP representation of the structure of **D-1** is shown in Fig. 1, together with the atomic numbering. Atomic coordinates are given in Table 1 and some representative bond lengths, bond angles and torsion angles are reported in Table 2. They show that the rotamer which crystallizes is the E isomer with an OC_1C_5P torsion angle close to zero (−1.8°). The structure is quite similar to that found for other benzophosphaalkenes: the benzene ring linked to the phosphaalkenic carbon is almost coplanar with the CC=P fragment and the corresponding plane is practically perpendicular to that of the phenyl ring linked to the phosphorus atom (−89.6°).

Atomic coordinates and displacement parameters, bond lengths, bond angles and torsional angles have been deposited at the Cambridge Crystallographic Data Centre, 12 Union Road, Cambridge CB2 1EZ, UK.

3.2. Isomerization

^{31}P NMR spectra show that immediately after recrystallization, only the E isomers of **1** and **2** are present in the samples. However, when the sample has been exposed to the radiation of a Hg lamp (5 min for **1**, 1 min for **2**), additional ^{31}P NMR signals appear (δ = 222.2 ppm for **1**, 224 ppm for **2**) and indicate that ca. 25% of **1** and 50% of **2** have been transformed into the Z isomer.

3.3. Electrochemistry

The voltammograms obtained with the phosphaalkenes **1** (Fig. 2) and **2** indicate that these compounds undergo one-electron reduction at the platinum electrode. The anodic and cathodic peak potential values measured in DMF with a scan rate of 50 mV s^{-1} are

Table 2
Selected bond lengths (Å), bond angles and torsional angles (°) for compound **D-1**

P–C(5)	1.673(2)	C(1)–C(2)	1.348(4)
P–C(6)	1.853(2)	C(1)–C(5)	1.439(3)
O–C(1)	1.364(3)	C(2)–C(3)	1.408(4)
O–C(4)	1.373(4)	C(3)–C(4)	1.302(5)
C(5)–D(5)	0.95(2)		
C(5)–P–C(6)	98.7(1)	C(1)–C(2)–C(3)	107.1(3)
C(1)–O–C(4)	105.8(2)	O–C(4)–C(3)	111.2(3)
O–C(1)–C(2)	109.1(2)	P–C(5)–C(1)	125.5(2)
O–C(1)–C(5)	117.6(2)	P–C(5)–D(5)	121(1)
C(2)–C(1)–C(5)	133.4(3)	C1–C(5)–D(5)	114(1)
C(2)–C(3)–C(4)	106.9(3)		
O–C(1)–C(5)–P	−1.8(3)	C(5)–P–C(6)–C(11)	−89.6(2)
C(2)–C(1)–C(5)–P	176.7(2)	C(6)–C(7)–C(12)–C(13)	35.9(3)
C(6)–P–C(5)–C(1)	−179.0(2)	C(8)–C(9)–C(16)–C(17)	−62.4(3)
C(5)–P–C(6)–C(7)	81.4(2)	C(10)–C(11)–C(20)–C(21)	23.2(3)

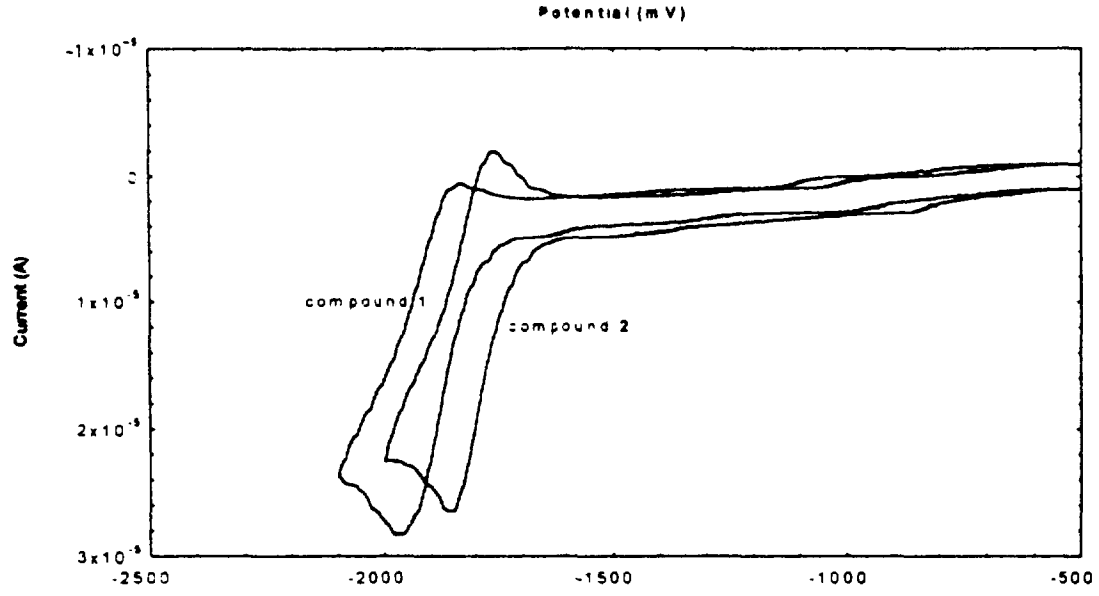

Fig. 2. Cyclic voltammogram (50 mV s^{-1}) of **1** and **2**, at a platinum electrode, in DMF with 0.10 M $^{n}Bu_4NPF_6$ electrolyte.

(a) for **1**: $E_p(a) = -1.84$ V vs. SCE and $E_p(c) = -1.97$ V vs. SCE ($E_{1/2} = -1.905$ V vs. SCE); (b) for **2**: $E_p(a) = -1.79$ V vs. SCE and $E_p(c) = -1.85$ V vs. SCE ($E_{1/2} = -1.82$ V vs. SCE). The fact that ΔE_p increases with scan rate is indicative of a quasi-reversible process for the reduction of both compounds.

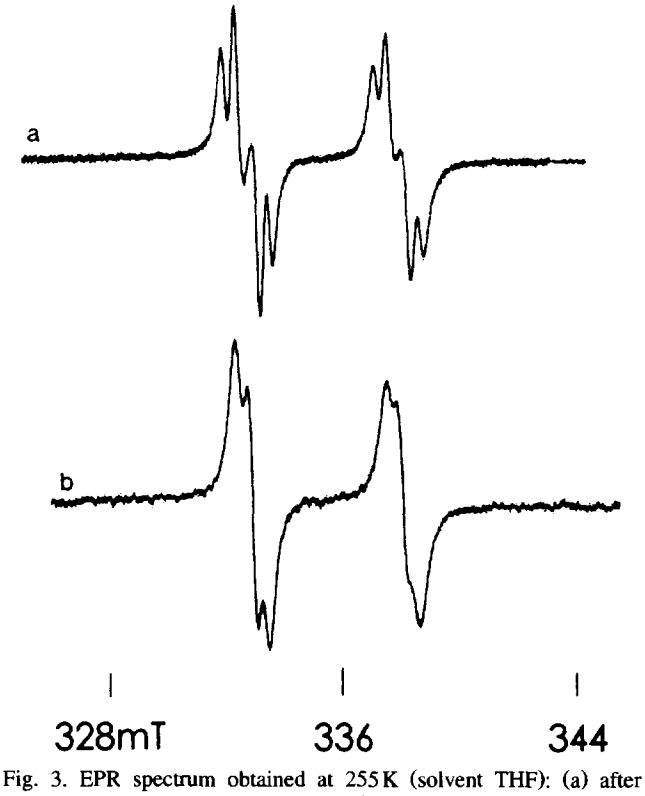

Fig. 3. EPR spectrum obtained at 255 K (solvent THF): (a) after reaction of **1** with a potassium mirror; (b) after reaction of **D-1** with a potassium mirror.

3.4. Electron paramagnetic resonance

Attempts to observe EPR signals by generating the radical anions electrochemically inside the EPR cavity were unsuccessful. As explained below, it was nevertheless possible to obtain EPR spectra by generating the radical anion chemically. When a colorless solution of **1** in THF was put into contact with a potassium mirror at 255 K it became yellow and gave rise to the spectrum shown in Fig. 3(a). Measurements at variable temperature showed that the radical anion was not stable above 255 K. The spectrum recorded at this temperature exhibits hyperfine coupling with four spin 1/2 nuclei. On decreasing the temperature the line widths broaden and finally, at 170 K, the frozen solution leads to the spectrum shown in Fig. 4. This spectrum is characteristic of an axial hyperfine coupling tensor with a spin 1/2 nucleus, the absence of a central line indicates that the perpendicular components are close to zero. Simulation of this spectrum leads to the hyperfine eigenvalues reported in Table 3. This tensor is totally consistent with an unpaired electron, mainly localized in a 3p orbital of a phosphorus atom. Assuming a positive sign for the three eigenvalues implies an isotropic coupling

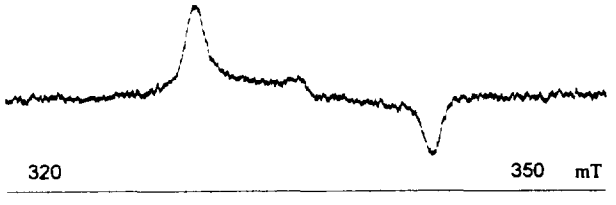

Fig. 4. Frozen solution EPR spectrum (170 K) obtained after reaction of **1** with a potassium mirror.

Table 3
Experimental EPR parameters for **1** and **2**

Radical anion	Liquid state						Solid state	
	g_{av}	^{31}P-A_{iso} (MHz)	^{1}H-A_{iso} (MHz)				g-tensor	^{31}P-tensor (MHz)
			A1	A2	A3	A4		
1^{-}	2.0052	145	13	12	11.5	4	$g_{\perp} = 2.0075$ $g_{\parallel} = 2.0006$	$T_{\perp} = 7$ $T_{\parallel} = 420$
2^{-}	2.0051	137	12.5	12	11.5	4	$g_{\perp} = 2.0061$ $g_{\parallel} = 2.0029$	$T_{\perp} = 8$ $T_{\parallel} = 394$

constant equal to 145 MHz. This value indicates that the largest splitting observed on the spectrum recorded at 255 K is due to ^{31}P. Replacement of the hydrogen atom bound to the phosphaalkene carbon by a deuterium atom leads, at 255 K, to the spectrum shown in Fig. 3(b), the disappearance of the 0.45 mT splitting indicates that the isotropic coupling with this proton is equal to 12.5 MHz. An excellent simulation of the spectrum is afforded by using the coupling constants reported in Table 3. The small 4 MHz constant is not resolved but is consistent with the experimental line width.

A colorless solution of **2** in THF turned to dark blue when reacting at 240 K with a potassium mirror and gave rise, at the same temperature, to an EPR spectrum characterized by a large hyperfine splitting of 4.9 mT and additional smaller couplings with three protons. Above 240 K the spectrum disappeared, below 220 K it broadened considerably. At 170 K the solution was frozen and a 'powder-like' spectrum similar to that recorded for $\mathbf{1}^{-\cdot}$ was obtained. Simulation of this latter spectrum led to the ^{31}P hyperfine eigenvalues shown in Table 3; the resulting isotropic coupling constant is totally consistent with the value (137 MHz) measured in the liquid phase. The spectrum recorded at 240 K was simulated by using the isotropic coupling constants given in Table 3. These values are quite similar to those obtained with **1** and, although we did not mark **2** with deuterium, it is reasonable to assume that the largest proton coupling is also due to the proton bound to the phosphaalkene carbon.

3.5. Ab initio calculations

Ab initio calculations (6 − 31 + G basis sets) have been performed on the model radical ions $\mathbf{1'}^{-\cdot}$ and $\mathbf{2'}^{-\cdot}$, where the bulky Ar group has been replaced by a hydrogen atom.

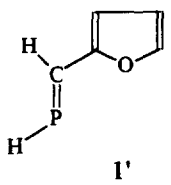

1'

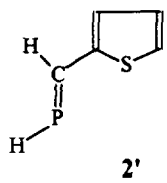

2'

Four planar structures are possible for each species (Fig. 5), and are characterized by the E/Z isomerization as well as the rotation around the C_1–C_5 bond (OC_1C_5P dihedral angle equal to 0° or 180°).

Optimizations of the structures of $\mathbf{1'}^{-\cdot}$ with the 6 − 31 + G basis set indicate that Z_{180} has the lowest energy, but this energy is only 0.3, 2.2 and 2.7 kcal mol^{-1} less than that of E_{180}, Z_0 and E_0 respectively. For the four isomers the SOMO is a π^* orbital formed by the p_π orbitals of the phosphaalkene group (ca. 76%) and the carbon p orbitals of the heterocycle (ca. 24%). There is almost no spin delocalisation on the oxygen atom. As shown in Table 4, the phosphorus spin density is slightly dependent upon the isomer: for E_{180} and Z_{180} this spin density is equal to 0.40, whereas it increases to 0.47 for Z_0 and E_0. In this same table we mention also the expectation value of the ^{31}P dipolar coupling calculated for each rotamer.

As shown in Table 4, the results obtained for the furane derivative are rather similar to those obtained for the thiophene-containing compound: the four rotamers of $\mathbf{2'}^{-\cdot}$ have practically the same energy (the energy of Z_{180} is 0.15 kcal, 1.3 kcal and 1.7 kcal less than that of

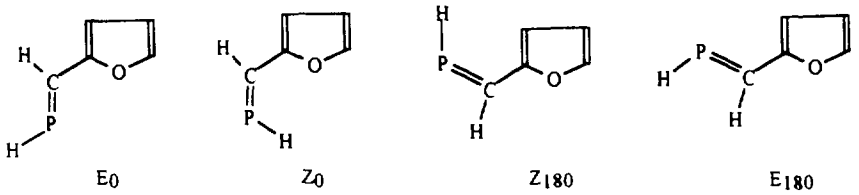

E_0 Z_0 Z_{180} E_{180}

Fig. 5. Representation of the four planar rotamers for **1**.

Table 4
Calculated atomic spin densities for the various rotamers of $\mathbf{1'}^{-\cdot}$ and $\mathbf{2'}^{-\cdot}$

Atom	Ion	Rotamers E_{180} and Z_{180}	Rotamers E_0 and Z_0
P	$\mathbf{1'}^{-\cdot}$	0.40	0.47
dipolar coupling (MHz)		166, −81, −85	199, −98, −101
	$\mathbf{2'}^{-\cdot}$	0.41	0.42
dipolar coupling (MHz)		171, −84, −87	174, −86, −88
C5	$\mathbf{1'}^{-\cdot}$	0.36	0.30
	$\mathbf{2'}^{-\cdot}$	0.28	0.27
C1	$\mathbf{1'}^{-\cdot}$	0.04	0.04
	$\mathbf{2'}^{-\cdot}$	0.04	0.04
C2	$\mathbf{1'}^{-\cdot}$	0.13	0.11
	$\mathbf{2'}^{-\cdot}$	0.17	0.15
C3	$\mathbf{1'}^{-\cdot}$	0.00	0.00
	$\mathbf{2'}^{-\cdot}$	0.00	0.00
C4	$\mathbf{1'}^{-\cdot}$	0.05	0.06
	$\mathbf{2'}^{-\cdot}$	0.06	0.07
heteroatom	$\mathbf{1'}^{-\cdot}$	0.01	0.02
	$\mathbf{2'}^{-\cdot}$	0.03	0.04

E_{180}, Z_0 and E_0 respectively) and ca. 30% of the unpaired electron is delocalized on the heterocycle.

4. Discussion

In contrast to phosphaalkenes that contain no aromatic ring linked to the P=C bond, **1** and **2** undergo quasi-reversible reduction. Replacement of the benzene ring by a furane and a thiophene ring slightly decreases the reduction potential of the phosphaalkene compounds, which passes from −1.98 V to −1.90 and −1.82 V. For the heterocycle-containing phosphaalkene the stability of the corresponding radical anions is, however, very low, and their EPR spectra could be observed only after reduction of the precursor with metallic potassium.

In order to estimate the phosphorus spin densities for $\mathbf{1}^{-\cdot}$ and $\mathbf{2}^{-\cdot}$, we have decomposed the ^{31}P hyperfine constants measured in frozen solution into isotropic A_{iso} and anisotropic τ_{aniso} coupling constants (see Table 5). Comparison of these values with the atomic constants [23] associated with an electron confined to a 3s and a 3p phosphorus orbital leads to the spin densities shown in Table 5. The spin densities on the various carbon atoms have been roughly estimated by using the usual McConnell relation and a corresponding Q value equal to 60 MHz. For the phosphaalkenyl carbon, the resulting values are 0.22 and 0.21 for the furane and the thiophene derivatives respectively. The spin densities on the carbon of the heterocycle are 0.2, 0.19 and 0.07 for both radical anions $\mathbf{1}^{-\cdot}$ and $\mathbf{2}^{-\cdot}$. These values are consistent with an unpaired electron delocalized in a π^* orbital built from the five-membered ring and the phosphaalkene double bond. The participation of the phosphaalkene moiety in this molecular orbital is equal to ca. 60%. These results are quite consistent with the values predicted by ROHF calculations, and indicate that the phosphorus spin densities are comprised between 0.40 and 0.47 for $\mathbf{1'}^{-\cdot}$ and between 0.41 and 0.42 for $\mathbf{2'}^{-\cdot}$. Owing to the anti-bonding character of the SOMO, it is plausible that a rapid exchange occurs in solution between the various rotamers, and the coupling values measured in the liquid phase certainly result from an averaging process. The observed ^{31}P isotropic coupling is mainly due to inner shell polarization. For the diphenylphosphine [24] a phosphorus p-spin density of 0.70 gives rise to an isotropic hyperfine interaction of 252 MHz; this implies averaged ^{31}P-A_{iso} values of 157 MHz and 148 MHz for $\mathbf{1}^{-\cdot}$ and $\mathbf{2}^{-\cdot}$ respectively, in very good accord with the experimental values (Table 5). However, the role of the bulky group Ar in the internal rotation process is probably crucial, and precludes a precise comparison between the experimental values and the couplings predicted for the model radical anions $\mathbf{1'}^{-\cdot}$ and $\mathbf{2'}^{-\cdot}$. The expectation value of the dipolar coupling for these two model radical anions (Table 5) are slightly less than the anisotropic couplings measured on $\mathbf{1}^{-\cdot}$ and $\mathbf{2}^{-\cdot}$ at 170 K.

It is worthwhile mentioning that both radical anions $\mathbf{1}^{-\cdot}$, $\mathbf{2}^{-\cdot}$ as well as the benzene phosphaalkene have similar spin delocalization on the phosphaalkene double bond, and the decrease in the ^{31}P isotropic coupling brought about by passing from the benzene (152 MHz) to the furane (145 MHz) and to the thiophene derivative (137 MHz) remains small when compared with the atomic constant (13 300 MHz).

Table 5
Experimental ^{31}P isotropic and anisotropic hyperfine couplings and spin densities

Radical anion	^{31}P-A_{iso} (MHz)	Anisotropic coupling constants		Phosphorus spin densities	
		$\tau_\perp$	$\tau_\parallel$	ρ_s	ρ_P
$\mathbf{1}^-$	144.5	−138	276	0.01	0.38
$\mathbf{2}^-$	137	−128.5	257	0.01	0.35

Acknowledgements

We thank the Swiss National Fund for financial support.

References

[1] Th.C. Klebach, R. Lourens and F. Bickelhaupt, *J. Am. Chem. Soc., 100* (1978) 4886.
[2] G. Bertrand, C. Couret, J. Escudié, S. Majid and J.P. Majoral, *Tetrahedron Lett., 23* (1982) 3567.
[3] A. Marinetti and F. Mathey, *Angew. Chem., Int. Ed. Engl., 27* (1988) 1382.
[4] M. Van der Sluis, J.B.M. Wit and F. Bickelhaupt, *Organometallics, 15* (1996) 174.
[5] M. Yoshifuji, K. Toyota and N. Inamoto, *Tetrahedron Lett., 26* (1985) 1727.
[6] F. Mercier, C. Hugel-Le Goff and F. Mathey, *Tetrahedron Lett., 30* (1989) 2397.
[7] R. Appel, in M. Regitz and O.J. Scherer (eds.), *Multiple Bonds and Low Coordination in Phosphorus Chemistry*, Thieme, Stuttgart, 1990, p. 157.
[8] G. Becker, W. Becker and O. Mundt, *Phosphorus and Sulfur, 14* (1983) 267.
[9] L.N. Markovskii and V.D. Romanenko, *Tetrahedron, 45* (1989) 6019.
[10] A.C. Gaumont and J.M. Denis, *Chem. Rev., 94* (1994) 1413.
[11] W.W. Schoeller, J. Niemann, R. Thiele and W. Haug, *Chem. Ber., 124* (1991) 417.
[12] M. Geoffroy, A. Jouaiti, G. Terron, M. Cattani-Lorente and Y. Ellinger, *J. Phys. Chem., 96* (1992) 8242.
[13] A. Jouaiti, M. Geoffroy, G. Terron and G. Bernardinelli, *J. Am. Chem. Soc., 117* (1995) 2251.
[14] R. Appel, J. Menzel, F. Knoch and P. Volz, *Z. Anorg. Allg. Chem., 534* (1986) 100.
[15] A.H. Cowley, J.E. Kilduff, J.G. Lasch, S.K. Mehrotra, N.C. Norman, M. Pakulski, B.R. Whittlesey, J.L. Atwood and W.E. Hunter, *Inorg. Chem., 23* (1984) 2582.
[16] M. Yoshifuji, I. Shima, N. Inamoto, K. Hirotsu and T. Higuchi, *J. Am. Chem. Soc., 103* (1981) 4587.
[17] E. Blanc, D. Schwarzenbach and H.D. Flack, *J. Appl. Crystallogr., 24* (1991) 1035.
[18] P. Main, S.J. Fiske, S.E. Hull, L. Lessinger, G. Germain, J.-P. Declercq and M.M. Woolfson, *A System of Computer Programs for the Automatic Solution of Crystal Structures from X-Ray Diffraction Data*, Universities of York, UK and Louvain-la-Neuve, Belgium, 1987.
[19] S.R. Hall, H.D. Flack and J.M. Stewart, XTAL3.2 *User's Manual*, Universities of Western Australia and Maryland, 1992.
[20] C.K. Johnson, ORTEP II, Report ORNL-5138, Oak Ridge National Laboratory, Oak Ridge, TN, 1976.
[21] M.J. Frisch, G.W. Trucks, H.B. Schlegel, P.M.V. Gill, B.G. Johnson, M.W. Wong, M.J.B. Foresman, M.A. Robb, M. Head-Gordon, E.S. Replogle, R. Gomperts, J.L. Andres, K. Raghavachari, J.S. Binkley, C. Gonzalez, R.L. Martin, D.J. Fox, D.J. Defrees, J. Baker, J.J.P. Stewart and J. Pople, Gaussian 92/DFT, Revision G.2, Gaussian Inc., Pittsburgh, PA, 1992.
[22] M.J. Frisch, G.W. Trucks, H.B. Schlegel, P.M.V. Gill, B.G. Johnson, M.A. Robb, J.R. Cheeseman, T. Keith, G.A. Petersson, J.A. Montgomery, K. Raghavachari, M.A. Al-Laham, V.G. Zakrzewski, J.V. Ortiz, J.B. Foresman, J. Ciolowski, B.B. Stefanov, A. Nanayakkara, M. Challacombe, C.Y. Peng, P.Y. Ayala, W. Chen, M.W. Wong, J.L. Andres, E.S. Reploges, R. Gomperts, R.L. Martin, D.J. Fox, J.S. Binkley, D.J. Defrees, J. Baker, J.P. Stewart, M. Head-Gordon, C. Gonzalez and J. Pople, Gaussian 94, Revision B.1, Gaussian Inc., Pittsburgh, PA, 1995.
[23] J.R. Morton and K.F. Preston, *J. Magn. Reson., 30* (1978) 577.
[24] M. Geoffroy, E.A.C. Lucken and C. Mazeline, *Mol. Phys., 28* (1974) 839.